2D.3 GOAL ORIENTED ADAPTIVITY FOR TROPICAL CYCLONES:
THE RESONANT INTERACTION OF A TROPICAL CYCLONE AND A TROPOPAUSE FRONT

Leonhard Scheck*[1], Sarah C. Jones[1], Martin Baumann[1], Vincent Heuveline[1], Martin N. Juckes[2]
[1] Karlsruhe Institute for Technology, Karlsruhe, Germany
[2] British Atmospheric Data Centre, Chilton, UK

1. INTRODUCTION

The development and motion of tropical cyclones (TCs) is influenced by processes on a large range of scales. Tropical cyclone motion is determined by the environmental flow on scales of several thousand kilometers whereas the genesis is particularly sensitive to inner-core convection on scales below several kilometers. The structure and intensification are influenced by the large-scale and the convective scale. Thus a multi-scale approach is essential to represent a tropical cyclone adequately.

Adaptive techniques are a promising way to tackle such challenging multi-scale problems. We are investigating techniques for automatic local mesh adaptation controlled by goal functionals. The sensitivity information obtained with goal oriented methods is used to refine the mesh automatically in a way that minimizes the error of the numerical solution with respect to an arbitrary physical quantity of interest. The sensitivity information presents not only a way to optimize the mesh, but can also provide insight into the processes that affect the development and motion of TCs.

In a joint mathematical-meteorological project we aim at applying goal-oriented techniques on problems related to tropical cyclones. Highly idealized TC scenarios are investigated, as the TC problem in its entirety is too complex and not sufficiently well understood to serve as a test problem. For this purpose we define barotropic TC problems that could benefit considerably from goal-oriented adaptivity. We perform non-adaptive high-resolution reference model runs for these scenarios which will be compared to adaptive calculations using different goal functionals.

In the following we will first give a short overview of the goal oriented approach and present first results for a barotropic problem studied by Schubert et al. (1999). Then we focus on a second scenario, the interaction of a tropical cyclone with frontal waves. This problem is relevant for the extratropical transition of tropical cyclones and shows an interesting sensitivity to changes in the initial state.

2. GOAL-ORIENTED ADAPTIVITY

The aim of the goal oriented approach investigated in this project is to adapt the mesh automatically in a way that minimizes the error of the numerical solution with respect to a given arbitrary physical quantity of interest, while keeping e.g. the number of grid points constant. The physical quantity is represented by a so-called goal functional J. An a posteriori error estimator is used to obtain the sensitivity information that indicates which parts of the mesh have the largest influence on the error in J.

Given a partial differential equation in variational formulation,

$$u \in V: \quad a(u,\varphi) = f(\varphi)$$

for all test functions $\varphi \in V$, we are interested in $J(u)$, where u is the exact solution of the problem. An approximate solution $u_h \in V_h \subset V$ can be calculated using the finite element method and allows us to compute an approximate value of the goal functional $J(u_h)$. Following the concept of the *Dual Weighted Residual (DWR) method* (Bangerth and Rannacher, 2003), the error $J(u) - J(u_h)$ that should be minimized can be written in terms of a residual expression

$$J(u) - J(u_h) = \rho(u_h, z - I_h(z)) + h.o.t.,$$

where $z \in V$ is the exact solution of the corresponding dual problem and $I_h(z) \in V_h$ a discrete interpolation. The dual problem is given by

$$z \in V: \quad \nabla_u a(u,z)\varphi = \nabla_u J(u)\varphi \quad \forall \varphi \in V.$$

In general the exact solution z of the dual problem is unknown. To estimate the error $J(u) - J(u_h)$ different approaches of approximating z by some Z can be applied, e.g. higher-order finite element solution, solution of local problems nested in a defect-correction iteration or patch-wise higher-order interpolation (see Bangerth and Rannacher (2003)). This allows us to estimate the error in the goal funtional,

$$J(u) - J(u_h) \approx \rho(u_h, Z - I_h(Z)) = \sum_{i=1..N} \eta_i, \qquad (1)$$

where the so-called local *error indicators* $\eta_i \geq 0$ represent each cell's contribution to the total error in J. Based on these local error indicators both the spatial mesh and the time steps can be adapted, e.g. by subdividing cells with a large contribution to the total error in J.

For time-varying applications the primal and dual problems are defined by

$$u \in V: \int_0^T (\partial_t u, \varphi)_\Omega + a(u,\varphi)\,\mathrm{d}t = \int_0^T f(\varphi)\,\mathrm{d}t,$$

$$z \in V: \int_0^T -(\partial_t z, \varphi)_\Omega + \nabla_u a(u,z)\varphi\,\mathrm{d}t = \nabla_u J(u)\varphi$$

for all $\varphi \in V$, where $(a,b)_\Omega := \int_\Omega a(x)\cdot b(x)\ \mathrm{d}x$ and Ω denotes the spatial domain. As the dual problem is posed

*Corresponding author address: Leonhard Scheck, Karlsruher Institut für Technologie, Institut für Meteorologie und Klimaforschung, 76128 Karlsruhe, Germany; e-mail: scheck@kit.edu

backwards in time and depends on the solution of the primal problem, it can be solved only after the solution of the primal problem is known. Thus obtaining a solution with the desired accuray requires an iterative process In each iteration step the primal problem is solved forward in time, then the dual problem is solved backward in time, and subsequently the error is estimated for each grid zone and the grid is adapted accordingly.

The solution of the dual problem for time-varying problems and the calculation of error estimates has been implemented in the finite element package *HiFlow3* (www.hiflow3.org/) and is now tested using TC-related problems. A first example (Fig. 1) is based on a barotropic problem investigated by Schubert et al. (1999). In this scenario a ring-shaped vorticity distribution representing the eyewall of a TC becomes unstable due to barotropic instability. In Fig. 1 the evolution of the primal and the dual solution are shown for a goal functional

$$J(u) := \int_\Omega \omega(x) u_1(x, T)\, \mathrm{d}\, x,$$

where ω is a weight function that is non-zero only in a small neighbourhood of a point x_0 within the domain, u_1 denotes the x-component of the velocity and $T = 7.25$h is the time at the end of the simulated time span. At $t = T$ the goal functional is sensitive only to the solution near point x_0 (lower right panel in Fig. 1). For $t < T$ perturbations located on the blueish spiral would have an effect on $u_1(x_0, T)$.

As a next step we will perform simulations, in which the grid is adapted during the simulation, using either the approach of Bangerth and Rannacher (2003) or alternatives that are computationally less expensive. We will also compare the sensitivity information given by the dual solution for different goal functionals with sensitivity information obtained by computing singular vectors. Furthermore, we will perform tests with other TC-scenarios like the one discussed in the following.

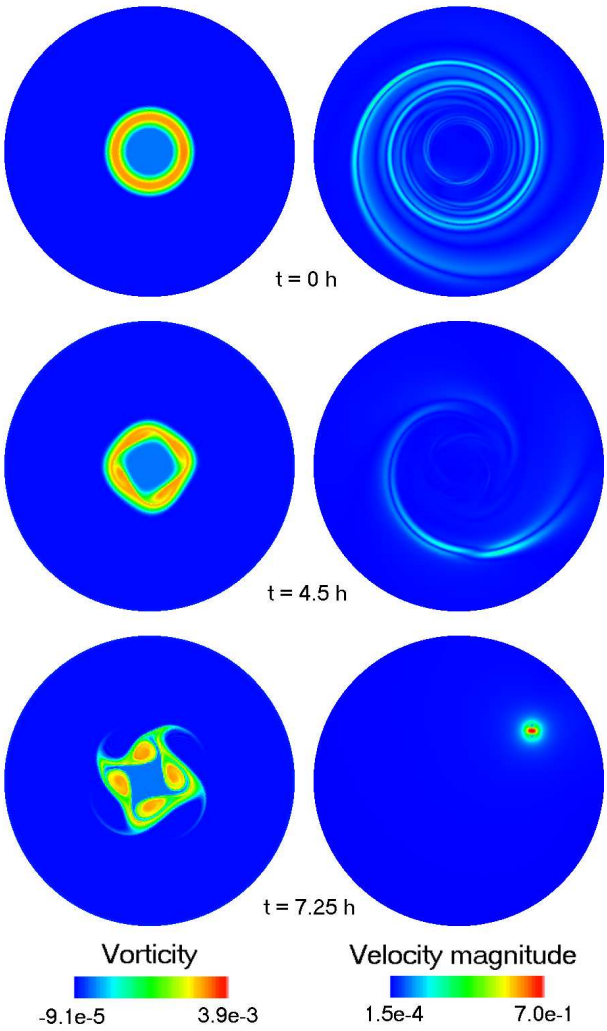

FIG. 1: Vorticity of the primal solution (left column) and absolute value of the velocity in the dual solution (right column) at the start and the end of the simulated time span and at an intermediate time for a problem studied by Schubert et al. (1999).

3. CYCLONE-FRONT INTERACTION

The barotropic instability in the problem presented above requires high resolution and could thus benefit substantially from local grid refinement. However, only scales less than about 100 km are important in this case, which does not involve any interaction with the large scale flow. The flow on scales of several 1000 km is decisive for the next scenario that we will use to test goal-oriented adaptivity techniques and which we have already investigated using non-adaptive methods.

The interaction between a TC and a tropopause front is a common process for TCs that encounter the mid-latitude flow and undergo extratropical transition. The circulation of the TC excites Rossby waves on the strong potential vorticity gradient in the upper troposphere that is associated with the jetstream. This has consequences for the motion, structure and intensity of the cyclone as well as for the downstream development. Furthermore, pre-existing frontal waves can also influence the tropical cyclone. In order to gain insight into these processes we study the problem in its most idealised configuration, using a nonlinear barotropic model (Scheck et al., 2010a; Scheck et al., 2010b). Analytic studies of the vortex-jet interaction (restricted to wave amplitudes smaller than the cyclone-jet separation) have been performed by Bell (1990) and numerical simulations of such processes, but in the context of the polar vortex, were performed by Schwierz et al. (2004).

3.1 *Model Description*

The velocity profile of a typical jetstream can be approximated in a barotropic beta-plane model by assuming piecewise constant absolute vorticity with a low value to the south a high value to the north and a jump at the front (Fig. 2). This can be interpreted as the tropopause

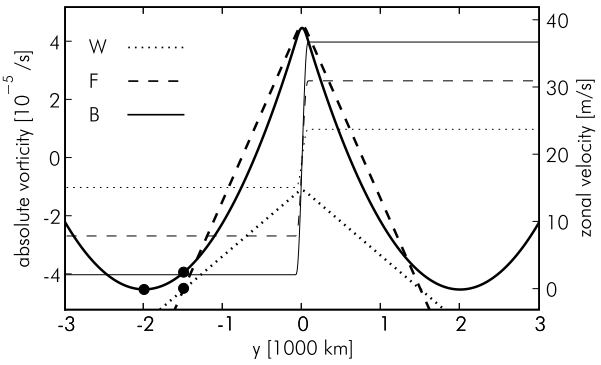

FIG. 2: Absolute vorticity (thin) and zonal velocity (thick) for the basic state with a vorticity jump $\eta_0 = 4 \times 10^{-5}s^{-1}$ on the β-plane (solid) and the basic states with $\eta_0 = 10^{-5}s^{-1}$ (dotted) and $\eta_0 = 8/3 \cdot 10^{-5}s^{-1}$ (dashed) on the f-plane.

front associated with the jet stream. An advantage of this simple representation is that analytic solutions for Rossby waves trapped on the vorticity jump exist and that the dispersion relation for these frontal waves is known (Schwierz et al., 2004).

We model the TC using vortices with purely positive relative vorticity profiles as well as vortices with a core of positive vorticity enclosed by a ring of negative vorticity. In the course of the simulation the latter is partially removed from the positive core by the background shear and forms two anticyclones. This allows us to study also the potential influence of the anticyclonic upper-level outflow that is present in real TCs on the cyclone-jet interaction. In the following we show results for a vortex with a maximum tangential wind of 40 m/s and a radius of maximum wind of 100km.

For our calculations the initial state is obtained by adding the relative vorticity field of a vortex to the absolute vorticity background representing the jet. The initial position of the cyclone is 1500 km south of the jet. We use a channel geometry with periodic boundaries in the zonal direction and walls at the meridional boundaries. The model runs are performed with a finite difference code that solves the equations of non-divergent barotropic flow in the streamfunction-vorticity formulation. A third-order upwind scheme is used to compute the advection terms in combination with a second-order Runge-Kutta step for the time integration and the streamfunction is computed in Fourier space.

3.2 *Zonally Aligned Fronts*

The basic processes that govern the cyclone-jet interaction in all of our model runs are visible in Fig. 3, which shows the evolution of the absolute vorticity distribution for one representative case. Within several days the shear of the background flow removes fluid with negative relative vorticity from the cyclone, leading to the formation of two anticyclones. The circulation of the cyclone

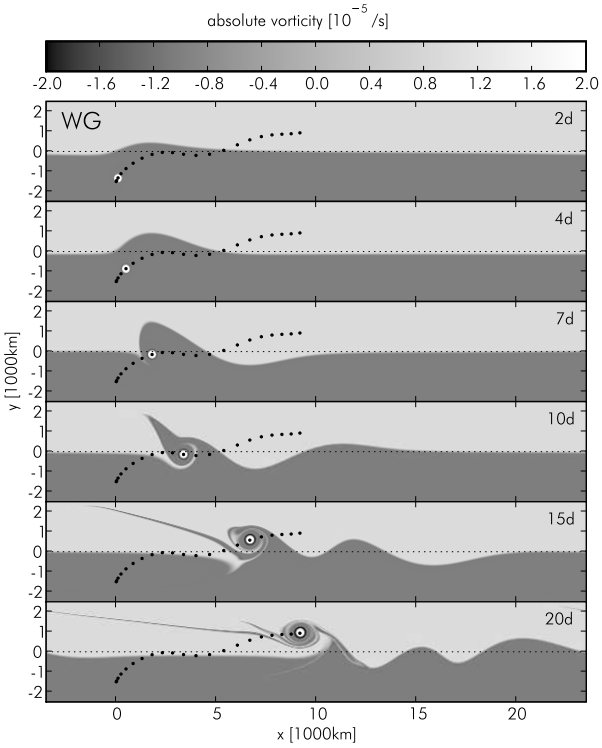

FIG. 3: Vorticity distribution 2, 4, 7, 10, 15 and 20 days after the start of a calculation with an initially unperturbed front. The black dots mark the cyclone position after every full day.

displaces the interface between the two regions of constant absolute vorticity, thereby generating a trough upstream and a ridge downstream of the cyclone. The vorticity anomalies associated with the trough and the ridge induce a circulation that advects the cyclone towards the jet (Fig. 4). Due to the faster background flow close to the vorticity interface the zonal translation speed of the cyclone increases. The ridge downstream of the cyclone grows much faster than the upstream trough (see Fig. 3, t=4d), because the circulations associated with the vorticity anomalies at the interface and the cyclone are parallel downstream and antiparallel upstream of the cyclone (see Fig. 4). In some model runs the downstream anticyclone contributes significantly to the growth of the ridge and the next trough further downstream (e.g. in the runs shown in Fig. 3 at around t=7d). When the cyclone reaches the jet, it moves into the the downstream ridge, starts to wind up the interface (see Fig. 3, $t > 7$ d) and is finally advected further northwards.

In most of the model runs the spectrum of the frontal waves excited during these processes is dominated by waves that are in resonance with the cyclone in the initial phase of the calculation. Resonant waves propagate with a phase speed that matches the zonal translation speed of the cyclone. A continuous interaction is possible only for waves that are close to resonance. The resonance

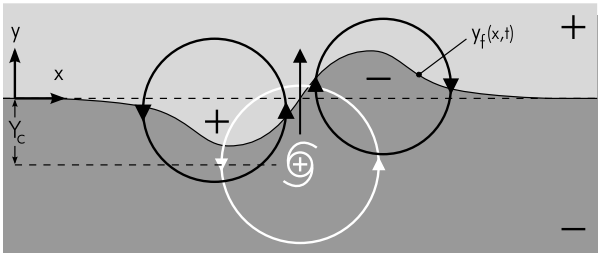

FIG. 4: The circulation induced by a cyclone (white circle) displaces the interface between an area of negative (dark gray) and positive (light gray) absolute vorticity. Two vorticity anomalies are created at the interface with associated circulations (black circles and arrows) that advect the cyclone towards the front.

condition is particularly important for high jet speeds, for which the phase speed changes more quickly with the wavelength, so that only a small range of wavelengths is close to resonance. For relatively slow jets, however, a larger range of wavelengths can contribute to the interaction and the cyclone circulation is able to perturb the jet more strongly. The strength of the cyclone-jet interaction is also influenced by another effect that depends on the jet velocity: For a given wave amplitude the circulation induced by the wave increases with the jet speed, thus enhancing the impact on the cyclone motion. In general the latter effect is more important and thus the cyclone-jet interaction is enhanced for faster jet speeds.

3.3 *Pre-existing Frontal Waves*

A more realistic scenario for extratropical transition is the interaction of a cyclone with a jet that has already been perturbed by pre-existing frontal waves. In this case the resonant wavelength again plays an important role. While non-resonant waves have only a weak influence on the cyclone motion, resonant waves can modify the cyclone track considerably. The influence of a frontal wave depends on the phase of the wave with respect to the cyclone, which is defined as $\phi = \pi(X_c - X_0)/\lambda$, where λ is the wavelength of the frontal wave, X_c is the meridional coordinate of the cyclone and X_0 is the first point upstream ($X_0 < X_c$) of the cyclone where $y_f = 0$ and $\mathrm{d}y_f/\mathrm{d}x > 0$ (see Fig. 4). For $\phi = 0$, the situation shown in Fig. 4, the frontal wave enhances the northward advection of the cyclone. For phases around $\phi = \pi$ an initial southward advection of the cyclone results.

The cyclone track can depend strongly on the phase of the resonant wave. Figure 5 displays the time evolution of the meridonal and the zonal coordinate of the cyclone center for runs with different initial wave phases ϕ. The wave amplitude is 250 km, the wavelength 5400 km and the jet speed 40 m/s in all cases. Not surprisingly, for $\phi = 0$ (the case shown in Fig. 4), the cyclone is advected towards the jet faster than in the same model run without pre-existing frontal waves (Fig. 5, upper panel). In the model run with the inverse configuration ($\phi = 1.0\pi$), the

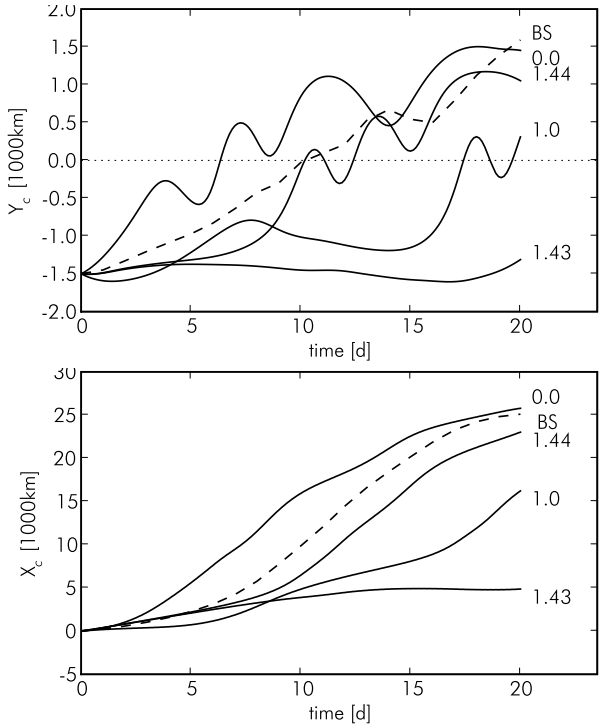

FIG. 5: Evolution of the meridional (top panel) and zonal (bottom panel) cyclone coordinate for model runs with inital wave phase $\phi/\pi = 0.0, 1.0, 1.43$ and 1.44 (solid lines) and the corresponding model run without pre-existing frontal wave (dashed line).

cyclone is initally advected southwards and stays south of the jet ($Y_c < 0$) for a much longer time.

An unexpected sensitivity to the initial conditions is found when comparing the runs with $\phi = 1.43\pi$ and $\phi = 1.44\pi$ that are also shown in Fig. 5. The only difference in the inital conditions of these two model runs is that the pre-existing frontal wave is shifted by $\lambda_5 \times 0.01 = 54$ km in zonal direction. Yet, after about five days the meridional locations of the cyclones in the two runs diverge dramatically. While for $\phi = 1.43\pi$ the cyclone moves southwards, it is advected rapidly northwards for $\phi = 1.44\pi$ and crosses the front at about the same time as in the unperturbed case. The huge differences in the temporal evolution of the meridional cyclone coordinate lead also to vastly different zonal cyclone positions (Fig. 5, lower panel). For $t > 9$ d the distance between the cyclones in the two cases grows by about 2000 km per day. Thus a extremely small perturbation in the inital state can cause the subsequent evolution completely.

The bifurcation of the cyclone tracks observed in the model runs takes place close to a point on the trough axis. To investigate the origin of this bifurcation it is helpful to make the simplifying assumption that the cyclone is steered only by the flows associated with the jet and the pre-existing frontal wave and that the influence of frontal waves excited by the cyclone can be neglected.

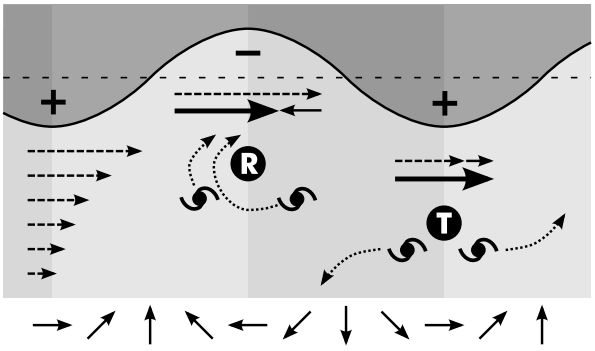

FIG. 6: Schematic view of the flow steering the cyclone in the presence of a frontal wave. The thin, solid arrows at the bottom indicate the direction of the wave circulation (u_f, v_f) and where $v_f > 0$ the shading is lighter. The dashed arrows at the left side depict the background flow $\bar{u}$. At points R and T the sum of the background flow velocity and the wave induced flow velocity is equal to the phase speed c (thick solid arrows). Thin dotted arrows indicate cyclone tracks in the frame moving with the phase speed of the wave.

In Fig. 6 a schematic view of this steering flow is given. The bifurcation point (marked T) is located at a distance to the jet where the zonal translation speed of the cyclone matches the phase velocity of the wave. On the trough axis the meridional velocity component at the cyclone center caused by the wave is zero. Thus the cyclone remains at the same meridional position and therefore its zonal translation speed remains constant and equal to the phase speed of the wave. In the frame of reference of the wave this is a stationary situation – cyclone and wave move with the same zonal velocity and their separation remains constant. The cyclone can stay close to this position for a rather long time. Very small changes in the initial wave phase determine whether the cyclone eventually moves towards the next trough-ridge transition downstream of the trough, where it is attracted by the front, or towards the ridge-trough transition upstream of the trough, where it is repelled from the front. The fact that very small changes in the initial state determine which of two vastly different solutions will occur gives rise to the bifurcation.

There is a second point for which the zonal translation speed of the cyclone matches the phase speed of the wave and the meridional translation speed is zero (point R in Fig. 6). However, the flow around this point, which is located on the ridge axis and close to the jet, tends to steer cyclones along the same tracks revolving around point R. The influence of the two points can be clearly seen in the upper panel of Fig. 7, which displays the cyclone tracks for about 50 model runs with initial wave phases ϕ bewteen 0 and 2π in the frame comoving with the wave. Close to point T the tracks are diverging and tracks are revolving around point R. If the flow steering the cyclones was just given by the zonal background flow of the jet and the

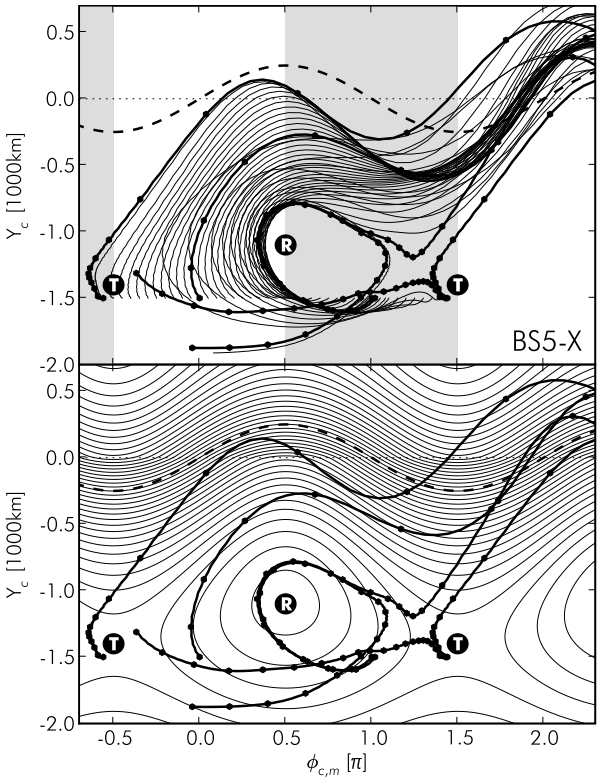

FIG. 7: *Upper panel:* Cyclone tracks (solid lines) in the frame moving with the phase speed c of the wave. For the cases ϕ/π = 1.0, 1.02, 1.43 and 1.44 thick lines are used and the start of each day is marked with a dot. The initial position of the cyclones is $Y_c = -1500$ km and the phase relative to the propagating wave, $\phi_c(t) = 2\pi(X_c(t) - c \cdot t)/\lambda$ is used as zonal coordinate. The dashed line is the pre-existing frontal wave. The location of points R and T (see Fig. 6) is indicated. *Lower panel:* The thick lines are the same as in the upper panel, the thin lines are stream lines for the flow due to the jet profile and the circulation of the pre-existing frontal wave in the frame moving with the wave.

flow caused by the propagating, pre-existing frontal wave, the cyclone should follow the stream lines of this flow like passive tracer particles. These streamlines are displayed in the lower panel of Fig. 7, together with some of the cyclone tracks. The tracks and the streamlines share some similarities, in particular also the streamlines diverge near point T and there are closed streamlines around point R.

However, clear differences are visible. The deviation of the tracks from the streamlines in the initial phase and the fact that the bifurcation takes place slightly upstream of point T are caused by the vortex profile used for these model runs. The vortex model contains negative vorticity in its outer regions, which is partly sheared from the positive core in the first few days and has some influence on the cyclone motion during this process. The second reason for the differences between tracks and streamlines

are the additional frontal waves excited by the cyclones during the simulation, which become stronger with time and cannot be neglected any more when the cyclone is close to the front. For weaker cyclones or stronger pre-existing frontal waves the tracks would stay closer to the streamlines for a longer time.

Several other sets of model runs (see Scheck et al. (2010b)) with different inital wave phases demonstrate that the bifurcations are in general not suppressed when additional wave modes are exited. Furthermore, these model runs show that only for a limited range of wavelengths (about 3000 – 6000 km for the setup considered above) bifurcations are possible and that the largest effect are obtained for the longest wavelengths of this range.

3.4 *Cyclone-Jet Interaction as a Test Problem for Adaptivity*

Due to the large range of scales involved in this problem from the cyclone structure (several tens of kilometres) to large scale waves ($>$ 10000 km) adaptive techniques could be very useful for this scenario. In particular, using goal oriented adaptivity could prove advantageous, as this method should allow us to determine which of the (in general many) frontal waves will become resonant at some point in time and have a large influence on the cyclone track. This is not possible for most adaptivity approaches. By choosing a goal functional that is sensitive to the cyclone motion, the grid will automatically be refined in a way that optimizes the representation of these waves and all processes that excite or modify them.

Furthermore, this scenario provides the opportunity to study the influence of a bifurcation on the sensitivity analysis that is part of the goal-oriented approach and on other methods like singular vectors.

Acknowledgements

This work is supported by the Deutsche Forschungsgemeinschaft (DFG-SPP 1276 Metström).

REFERENCES

Bangerth, W. and R. Rannacher, 2003: *Adaptive finite element methods for differential equations*. Birkhäuser Verlag.

Bell, G. I., 1990: Interaction between vortices and waves in a simple model of geophysical flow. *Physics of Fluids A: Fluid Dynamics*, **2**(4), 575–586.

Scheck, L., S. C. Jones, and M. Juckes, 2010a: The resonant interaction of a tropical cyclone and a tropopause front in a barotropic model, part i: Zonally-oriented front. *J. Atmos. Sci.* submitted.

Scheck, L., S. C. Jones, and M. Juckes, 2010b: The resonant interaction of a tropical cyclone and a tropopause front in a barotropic model, part ii: Frontal waves. *J. Atmos. Sci.* submitted.

Schubert, W. H., M. T. Montgomery, R. K. Taft, T. A. Guinn, S. R. Fulton, J. P. Kossin, and J. P. Edwards, 1999: Polygonal eyewalls, asymmetric eye contraction, and potential vorticity mixing in hurricanes. *Journal of the Atmospheric Sciences*, **56**(9), 1197–1223.

Schwierz, C., S. Dirren, and H. C. Davies, 2004: Forced waves on a zonally aligned jet stream. *J. Atmos. Sci.*, **61**(1), 73–87.